FTIR Study of the Retinal Schiff Base and Internal Water Molecules of Proteorhodopsin†

Daisuke Ikeda, Yuji Furutani, and Hideki Kandori*

Department of Materials Science and Engineering, Nagoya Institute of Technology, Showa-ku, Nagoya 466-8555, Japan

Received January 24, 2007; Revised Manuscript Received March 2, 2007

ABSTRACT: Proteorhodopsin (PR), an archaeal-type rhodopsin found in marine bacteria, is a light-driven proton pump similar to bacteriorhodopsin (BR). It is known that Asp97, a counterion of the protonated Schiff base, possesses a higher pK_a (∼7) compared to that of homologous Asp85 in BR (<3). This suggests that PR has a hydrogen-bonding network different from that of BR. We previously reported that a strongly hydrogen-bonded water molecule is observed only in the alkaline form of PR, where Asp97 is deprotonated (Furutani, Y., Ikeda, D., Shibata, M., and Kandori, H. (2006) *Chem. Phys. 324*, 705−708). This is probably correlated with the pH-dependent proton pumping activity of PR. In this work, we studied the water-containing hydrogen-bonding network in the Schiff base region of PR by means of Fourier-transform infrared (FTIR) spectroscopy at 77 K. [ζ-^{15}N]Lys-labeling and ^{18}O water were used for assigning the Schiff base N−D and water O−D stretching vibrations in D_2O, respectively. The frequency upshift of the N−D stretch in the primary K intermediate is much smaller for PR than for BR, indicating that the Schiff base forms a hydrogen bond after retinal photoisomerization. We then measured FTIR spectra of the mutants of Asp97 (D97N and D97E) and Asp227 (D227N and D227E) to identify the amino acid interacting with the Schiff base in the K state. The PR_K minus PR spectra of D97N and D97E were similar to those of the acidic and alkaline forms, respectively, of the wild type implying that the structural changes upon retinal photoisomerization are not influenced by the mutation at Asp97. In contrast, clear spectral differences were observed in D227N and D227E, including vibrational bands of the Schiff base and water molecules. It is concluded that Asp227 plays a crucial role during the photoisomerization process, though Asp97 acts as the primary counterion in the unphotolyzed state of PR.

Molecular pumps are membrane proteins that actively transport ions. Bacteriorhodopsin (BR[1]), a light-driven proton pump in *Halobacterium salinarum*, is the best studied molecular pump, whose tertiary structure and proton pathway have been determined (*1*, *2*). Light causes photoisomerization of the retinal chromophore from the all-*trans* to 13-*cis* form. The primary proton transfer from the protonated retinal Schiff base to Asp85 initiates the sequential proton-transfer reactions in BR. Consequently, one proton is translocated by a single photon absorption. It is generally accepted that a negatively charged aspartate (Asp85) and its transient protonation (formation of the M intermedate) are necessary for the pumping function of BR. A water molecule bridges the Schiff base and Asp85, whose hydrogen-bonding alteration is also important (*3*).

Recently, archaeal-type rhodopsins have also been discovered in eukaryotes (*4*, *5*) and eubacteria (*6*, *7*), which provided a good opportunity to understand the general molecular mechanism of proton pumping (*8*). One of the examples is proteorhodopsin (PR) found in various species of marine γ-proteobacteria (*9*−*11*). Because of the widespread distribution of proteobacteria in oceanic waters worldwide, this pigment may significantly contribute to the global solar energy input in the biosphere. Among thousands of PRs, the best studied protein is green PR (herein referred to as PR). The counterion of the Schiff base in PR is Asp97, and its pK_a is higher in PR (∼7) compared to that of homologous Asp85 in BR (2−3) (*12*, *13*). This indicates that Asp97 has a negative charge only at alkaline pH. There has been a debate on the pH dependence of the proton-pumping activity of PR. Two groups reported that only the alkaline form of PR pumps protons, whereas the acid PR does not (*12*, *14*, *15*). In contrast, another group reported that the alkaline and acid PRs pump protons by two-photon and single-photon absorption mechanisms with different vectoriality (*13*). Thus, the proton-pumping mechanism of PR is not understood completely, though the photocycle was well characterized (*16*, *17*).

We have studied the protein structural changes of various rhodopsins by means of Fourier-transform infrared (FTIR) spectroscopy (*18*). Earlier, we detected very low frequencies for water-stretching vibrations (O−D stretches at 2171, 2292, and 2323 cm^{-1} in D_2O) in BR, indicating that the water molecules form strong hydrogen bonds (*19*). By using mutant proteins, we have experimentally revealed that these water

† This work was supported in part by grants from Japanese Ministry of Education, Culture, Sports, Science, and Technology to H.K.

* To whom correspondence should be addressed. Phone/Fax: 81-52-735-5207. E-mail: kandori@nitech.ac.jp.

[1] Abbreviations: PR, proteorhodopsin; BR, bacteriorhodopsin; PR_K, K intermediate of PR; BR_K, K intermediate of BR; HOOP, hydrogen out-of-plane vibration; PC, L-α-phosphatidylcholine.

10.1021/bi700143g CCC: $37.00
Published on Web 04/12/2007

molecules participate in the hydrogen-bonding network in the Schiff base region of BR (*20*, *21*). Such FTIR observation is consistent with the X-ray structure of BR (*22*), and the vibrational frequencies are also consistent with the QM/MM calculations of the Schiff base region of BR (*23*). Subsequent studies of BR mutants and various rhodopsins have shown that strongly hydrogen-bonded water molecules are only found in the proteins exhibiting proton-pumping activity (*24*). These results suggested that strongly hydrogen-bonded water molecules and the transient weakening of their bonding are required for the proton-pumping function of rhodopsins. Previously, we measured FTIR spectra of PR under alkaline and acidic pH conditions, particularly focusing on the hydrogen-bonding conditions of internal water molecules (*25*). We observed highly pH-dependent spectra in the O−D and N−D stretching frequency region (in the 2700−2000 cm^{-1}) in D_2O, though the FTIR spectra were similar between pH 10 and 5 in the 1800−900 cm^{-1} region. A strongly hydrogen-bonded water molecule was observed only in the alkaline form of PR, which is consistent with the proton-pumping activity of PR at alkaline pH (*25*).

Such pH-dependence is due to the structural alteration by the protonation of Asp97, and the higher pK_a of Asp97 of PR compared to that of Asp85 of BR implies different hydrogen-bonding networks. In fact, it has been reported that the mutation of Asp97 in PR is less perturbing than that of Asp85 in BR (*26*), suggesting that the interaction between the retinal chromophore and Asp97 is weak. Nevertheless, a proton is transferred from the Schiff base to Asp97 during the pumping process of PR (*12*). What is the structure of the Schiff base region in PR? How different is the hydrogen-bonding network in the Schiff base region between PR and BR? Although there is no three-dimensional structure of PR at this moment, FTIR spectroscopy is a powerful tool to investigate the water-containing hydrogen-bonding network in rhodopsins (*3*, *18*). In this article, we studied structure and structural changes of PR by monitoring FTIR spectral changes at 77 K, where local structural changes around the retinal chromophore take place. We used [ζ-^{15}N]-Lys-labeling and ^{18}O water for assigning the Schiff base N−D and water O−D stretching vibrations in D_2O, respectively. In addition, we investigated the mutants of Asp97 (D97N and D97E) and Asp227 (D227N and D227E) to obtain detailed information about the structure and structural changes before and after retinal photoisomerization. The obtained spectral features were similar between the wild-type and the mutants of Asp97 but different for the mutants of Asp227. These results strongly suggest that Asp227 plays a crucial role during the photoisomerization process, though Asp97 acts as the primary counterion in the unphotolyzed state of PR.

MATERIALS AND METHODS

Preparation of the Proteorhodopsin Samples. The expression plasmids were constructed as described previously (*21*). For the mutants, we constructed a triple mutant in which all three cysteines (Cys-107, Cys-156, and Cys175 (*27*)) are replaced with serine as a starting template to avoid oxidation of one or more of the cysteine residues, followed by additional mutation at position 97 or 227. For the preparation of the expression plasmids of the mutants, a Quick-change site-directed mutagenesis kit (Stratagene) was used according to the stantdard protocol (*21*). The PR proteins possessing a six histidine tag at the C-terminus were expressed in *E. coli*, solubilized with 0.1% *n*-dodecyl β-D-maltoside (DM), and purified by Ni-column chromatography as described previously (*28*). [ζ-^{15}N]Lys-labeled PR was prepared according to the method described previously (*29*). The chromophore configurations of the PR samples were examined by using HPLC column chromatography (*30*), which showed that all proteins almost exclusively have all-*trans*-retinal.

FTIR Spectroscopy. Low-temperature FTIR spectroscopy was performed as described previously (*31*). For the FTIR measurements, the PR samples were reconstituted into L-α-phosphatidylcholine (PC) liposomes (PR/PC molar ratio of 1:50), where DM was removed by gently stirring with detergent-adsorbing Biobeads (100 mg of Biobeads/mg of protein; Bio-Rad). The PRs in the PC liposomes were washed three times with a buffer at pH 10.0 (alkaline form of the wild type), pH 5.0 (acidic form of the wild type), or pH 9.0 (D97N, D97E, D227N, and D227E mutants). Then, 100 μL of the PR sample was dried on a BaF_2 window with a diameter of 18 mm. After hydration by placing about 1 μL of H_2O, D_2O, or $D_2{}^{18}O$ beside the dry films and sealing with a silicon rubber O-ring and another BaF_2 window, the sample was placed in a cell, which was mounted in an Oxford DN-1704 cryostat in the Bio-Rad FTS-40 spectrometer. Illumination with 460 nm light at 77 K for 2 min converted PR to PR_K, and subsequent illumination with >640 nm light forced PR_K to revert to PR as described previously (*25*). The difference spectrum was calculated from the spectra constructed from 128 interferograms before and after the illumination. Fifty-six spectra obtained in this way were averaged to obtain the PR_K minus PR spectra. Because the samples in the films were randomly oriented, the IR polarizer was not used.

RESULTS

PR Mutants. It is known that the wild-type PR gradually loses its color after purification, but a triple cysteine mutant (TCM; C107S/C156S/C175S) is stable, suggesting that the instability originates from the oxidation of one or more of the three cysteine residues (Cys-107, Cys-156, and Cys175) (*27*). This was not a very serious problem for the FTIR measurements of the wild type (*25*), but we found it difficult to measure some mutant proteins. Therefore, in this study, we introduced mutations at position 97 or 227 into the TCM mutant PR but not into the wild type. It should be noted that the PR_K minus PR spectra were identical for the TCM and the wild-type PR (data not shown). Below, we describe each mutant protein with a single replacement, for example, D97N, not D97N/C107S/C156S/C175S, for the sake of simplicity.

The λ_{max} of D97N, D97E, D227N, and D227E were located at 548, 525, 523, and 508 nm in DM solution (pH 9), whereas those of the wild type and TCM were located at 523 nm (pH 9). The spectral red shift by 25 nm in D97N, but not in D227N, indicates that Asp97 is the principal counterion of the protonated Schiff base, as is the case in BR. In addition, the spectral blue shift in D227E by 15 nm suggests that Asp227 is also involved in the counterion

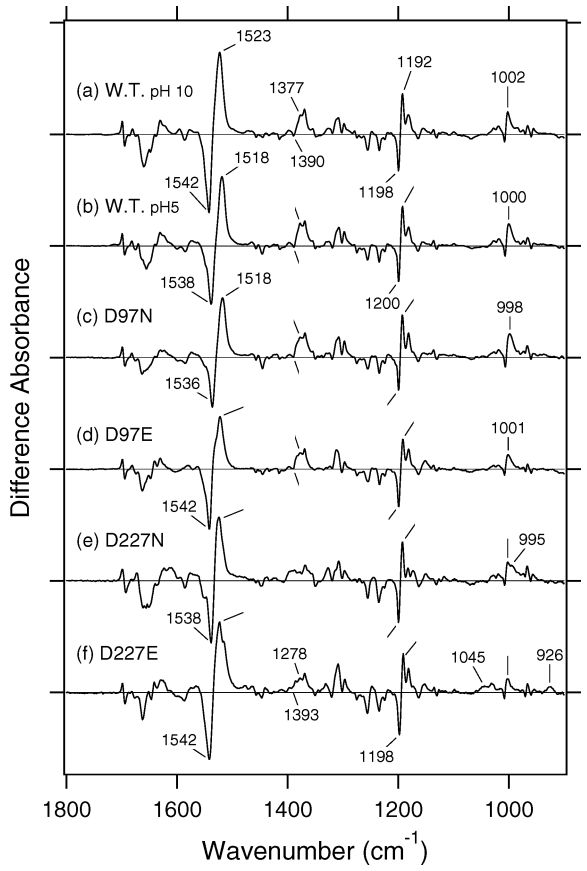

FIGURE 1: PR_K minus PR difference infrared spectra of the wild-type (pH 10; a, and pH 5; b), D97N (c), D97E (d), D227N (e), and D227E (f) PR in the 1800−900 cm^{-1} region. The mutant samples were prepared at pH 9. The samples were hydrated with H_2O, and spectra were measured at 77 K. The spectra in a and b are reproduced from Furutani et al. (*25*). One division of the *y*-axis corresponds to 0.007 absorbance units.

complex[2]. These features in UV−visible spectra suggest that both Asp97 and Asp227 act as Schiff base counterions, but Asp97 is more crucial. Such properties of the Schiff base region of PR resemble those of BR (*32*).

PR_K Minus PR Difference Infrared Spectra. Figure 1 shows the PR_K minus PR difference infrared spectra of the wild-type (pH 10; a, and pH 5; b), D97N (c), D97E (d), D227N (e), and D227E (f) PR in the 1800−900 cm^{-1} region. Because the pK_a of Asp97 in wild-type PR is around 7 (*12*), Figure 1a and b correspond to the spectra where Asp97 is deprotonated and protonated, respectively. The intense bands at 1542(−)/1523(+) cm^{-1} (a), 1538(−)/1518(+) cm^{-1} (b), 1536(−)/1518(+) cm^{-1} (c), 1542(−)/1518(+) cm^{-1} (d), 1538(−)/1518(+) cm^{-1} (e), and 1542(−)/1518(+) cm^{-1} (f) can be assigned to the ethylenic C═C stretching vibrations of the retinal chromophore. The lower frequency shift of the band indicates the formation of the red-shifted intermediate, PR_K, upon light absorption of PR at 77 K. It should be noted that the frequencies in mutants are not well correlated with the λ_{max} values, particularly for the mutants of Asp227. For instance, the λ_{max} of D227N and the wild type (pH 9) are identical (523 nm), but the C═C frequency is downshifted for D227N (1538 cm^{-1}; e) compared to that of the wild type (1542 cm^{-1}; a). The λ_{max} of D227E (508 nm) is blue-shifted compared to that of the wild type (523 nm), but the C═C frequency is identical for the wild type and D227E (1542 cm^{-1}; a and f).

Vibrational bands in the 1280−1050 cm^{-1} region can be assigned to the C−C stretching vibrations of the retinal chromophore, which monitor retinal configuration (*33*). The spectra in this frequency region resemble each other, though D227E shows a negative band at 1198 cm^{-1} (Figure 1f), not at 1200 cm^{-1}. The positive band at 1192 cm^{-1}, which was also reported in the previous resonance Raman study (*34*), shows that photoisomerization takes place from the all-trans to 13-cis form because the 1192 cm^{-1} band originates from the mixed C14−C15 and C10−C11 stretching vibrations of the 13-*cis*-retinal chromophore. In the case of BR, the band appears at 1194 cm^{-1} (*26*). An HPLC analysis showed that the wild-type and mutant proteins contain mostly all-*trans*-retinal in the dark (data not shown) so that the photoreaction of the 13-*cis* form is negligible in the present study.

Hydrogen-out-of-plane (HOOP) vibrations of the retinal chromophore appear in the 1000−900 cm^{-1} region, which is a good probe of the chromophore distortion after photoisomerization. Interestingly, spectral features of D97N (Figure 1c) and D97E (Figure 1d) are similar to those of the wild-type (Figure 1a and b) in the HOOP region, whereas those of the D227 mutants are considerably different. In fact, new peaks appeared at 995 cm^{-1} for D227N (Figure 1e), and at 1045 and 926 cm^{-1} for D227E (Figure 1f). A similar observation was made at 1400−1350 cm^{-1}, the frequency region of COO^- stretching vibrations of carboxylates, in which spectral features are different in the D227 mutants (Figure 1e and f). These observations strongly suggest that the mutations of Asp227 affect the structural changes in the PR-to-PR_K transition more significantly than those of Asp97. We will discuss each frequency region in detail below.

COO^- Stretching Vibrations of Carboxylates. Figure 2 shows the PR_K minus PR difference infrared spectra of the wild-type (pH 10; a, and pH 5; b), D97N (c), D97E (d), D227N (e), and D227E (f) PR in the 1440−1330 cm^{-1} region. The COO^- stretching vibrations of carboxylates appear in this frequency region. The bands at 1389(−)/1377(+) cm^{-1} of the wild type (Figure 2a and b) were preserved in D97N (Figure 2c) and D97E (Figure 2d). However, they disappear in D227N (Figure 2e) and seem to be shifting to 1393(−)/1378(+) cm^{-1} in D227E (Figure 2f). The most straightforward interpretation of the present observation is that the bands at 1389(−)/1377(+) cm^{-1} originate from the COO^- stretch of Asp227. In contrast, Asp97 and Glu97 both have the COO^- group, but their spectral features are similar, as shown in Figure 2a−d. These facts imply that the PR-to-PR_K transition does not involve structural changes at position 97, whereas structural changes occur at position 227. It is intriguing that retinal photoisomerization is accompanied by structural changes of Asp227, the minor counterion, but not by changes of Asp97, the principal counterion.

[2] We could argue from the identical λ_{max} for the wild type and D227N (523 nm) that Asp227 does not constitute the counterion complex in PR. The corresponding D212N mutant of BR exhibits a spectral red shift (*44*), indicating that Asp212 constitutes a counterion complex in BR. However, the results of D227E suggest that Asp227 influences the color tuning of PR. In addition, the D227N mutation affects the pK_a of Asp97 and the Schiff base, where Asp227 interacts with the Schiff base to a lesser extent than Asp97 (*30*, *43*). Therefore, Asp227 is probably involved in the hydrogen-bonding network of the Schiff base region and constitutes a conterion complex, as is the case for Asp212 in BR.

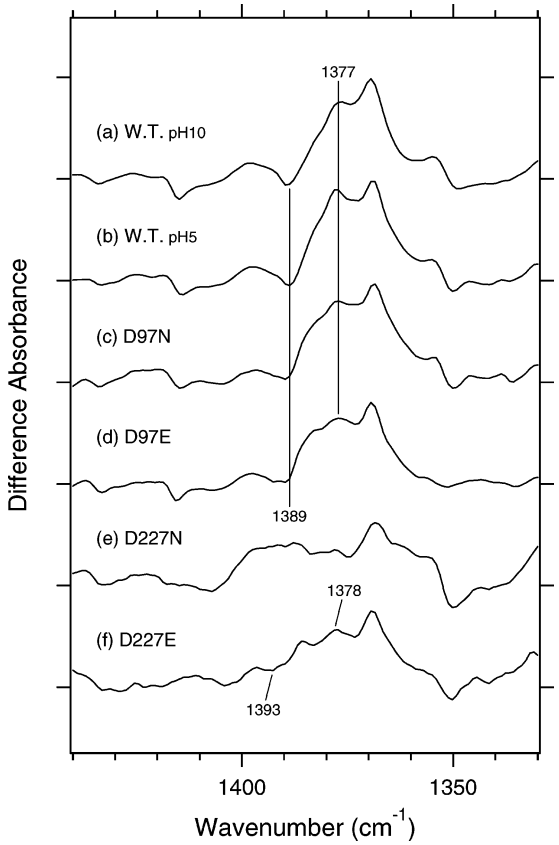

FIGURE 2: PR_K minus PR difference infrared spectra of the wild-type (pH 10; a, and pH 5; b), D97N (c), D97E (d), D227N (e), and D227E (f) PR in the 1440−1330 cm^{-1} region, which includes the COO^- stretching vibrations of carboxylates. The spectra are reproduced from Figure 1. One division of the *y*-axis corresponds to 0.0016 absorbance units.

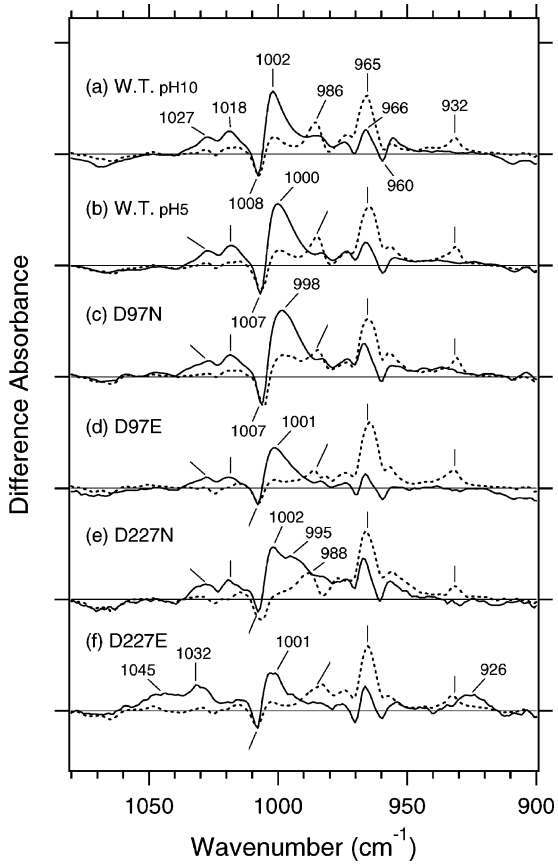

FIGURE 3: PR_K minus PR difference infrared spectra of the wild-type (pH 10; a, and pH 5; b), D97N (c), D97E (d), D227N (e), and D227E (f) PR in the 1080−900 cm^{-1} region, which corresponds to the hydrogen out-of-plane (HOOP) vibrations of the retinal choromophore. The samples were hydrated with H_2O (—) or D_2O (••••), and spectra were measured at 77 K. One division of the *y*-axis corresponds to 0.0025 units.

HOOP Vibrations of the Retinal Chromophore. Figure 3 shows the PR_K minus PR difference infrared spectra of the wild-type (pH 10; a, and pH 5; b), D97N (c), D97E (d), D227N (e), and D227E (f) PR in the 1080−900 cm^{-1} region. HOOP vibrations of the retinal chromophore appear in this frequency region, the marker band of the chromophore distortion, particularly after retinal photoisomerization (*35*, *36*). The H/D insensitive negative band at 1008 cm^{-1} in the wild type (Figure 3a) was assigned as the methyl rocking vibration, and the negative band at 960 cm^{-1} was also observed in the resonance Raman spectrum, presumably arising from the HOOP mode in PR (*34*). Positive peaks at 1027, 1018, and 1002 cm^{-1} exhibit spectral downshift upon hydration with D_2O, possibly to 986, 965, and 932 cm^{-1} (Figure 3a). Therefore, these bands can be attributed to the HOOP vibrations of the C15-H and/or N-H group. Similar spectra upon the protonation of Asp97 (pH 5, Figure 3b) and the mutation at position 97 (Figure 3c and d) show that the influence of structural modification of Asp97 is negligible. In contrast, clear spectral differences were seen for D227N and D227E. Figure 3e shows the appearance of a D_2O-sensitive new band at 995 cm^{-1} in D227N, which is attributable to the HOOP vibrations of the C15-H and/or N-H group. The positive bands at 1045 and 1032 cm^{-1} in Figure 3f are likely to be upshifted from 1027 and 1018 cm^{-1} in D227E, and a new band also appeared at 926 cm^{-1}. These results clearly demonstrate that the chromophore distortion upon PR_K formation is significantly affected by the mutations of Asp227 but not by the mutations of Asp97. Therefore, it is likely that Asp227 interacts with the retinal chromophore in the PR_K intermediate.

C═N Stretching Vibrations of the Retinal Chromophore and Amide-I Vibrations of Protein. Figure 4 shows the PR_K minus PR difference infrared spectra of the wild-type (pH 10; a, and pH 5; b), D97N (c), D97E (d), D227N (e), and D227E (f) PR in the 1770−1550 cm^{-1} region. Most bands in this frequency region are ascribable to vibrations of the protein except for the C═N stretching vibration of the choromophore in the 1650−1600 cm^{-1} region. The bands at 1699(+)/1695(−) cm^{-1} were previously assigned as the C═O stretching vibration of Asn230 (*26*). They were not influenced by mutations of Asp97 and Asp227 (Figure 4c−f).

The H/D sensitive negative band at 1660 cm^{-1} in H_2O (at 1636 cm^{-1} in D_2O) can be assigned as the C═N stretch of the chromophore (Figure 4a). The frequency upshift in H_2O is caused by coupling to the N−H bending vibration of the Schiff base, and the difference in frequency between H_2O and D_2O has been regarded as a measure of the hydrogen-bonding strength of the Schiff base (*37*). The positive band was also observed at 1631 and 1602 cm^{-1} in H_2O and D_2O, respectively, presumably due to the C═N stretch of PR_K (Figure 4a). The differences in frequencies were similar for PR_K (29 cm^{-1}) and PR (24 cm^{-1}), suggesting similar hydrogen-bonding strengths of the Schiff base before and

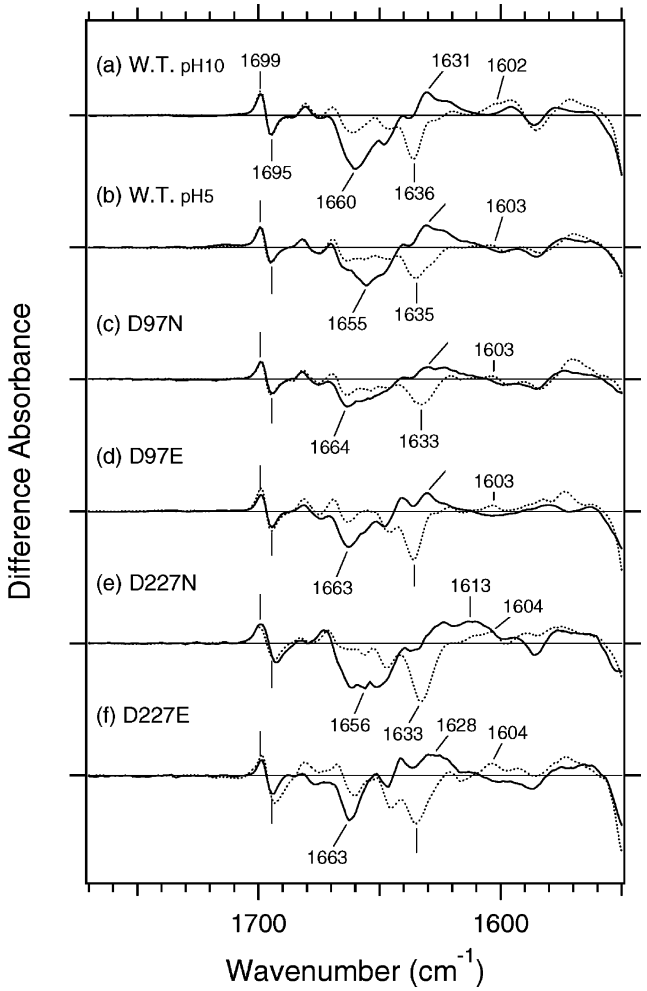

FIGURE 4: PR_K minus PR difference infrared spectra of the wild-type (pH 10; a, and pH 5; b), D97N (c), D97E (d), D227N (e), and D227E (f) PR in the 1770−1550 cm^{-1} region. Most bands in this frequency region are ascribable to protein vibrations except for the C═N stretching vibration of the choromophore. The samples were hydrated with H_2O (—) or D_2O (····), and spectra were measured at 77 K. One division of the *y*-axis corresponds to 0.0004 units.

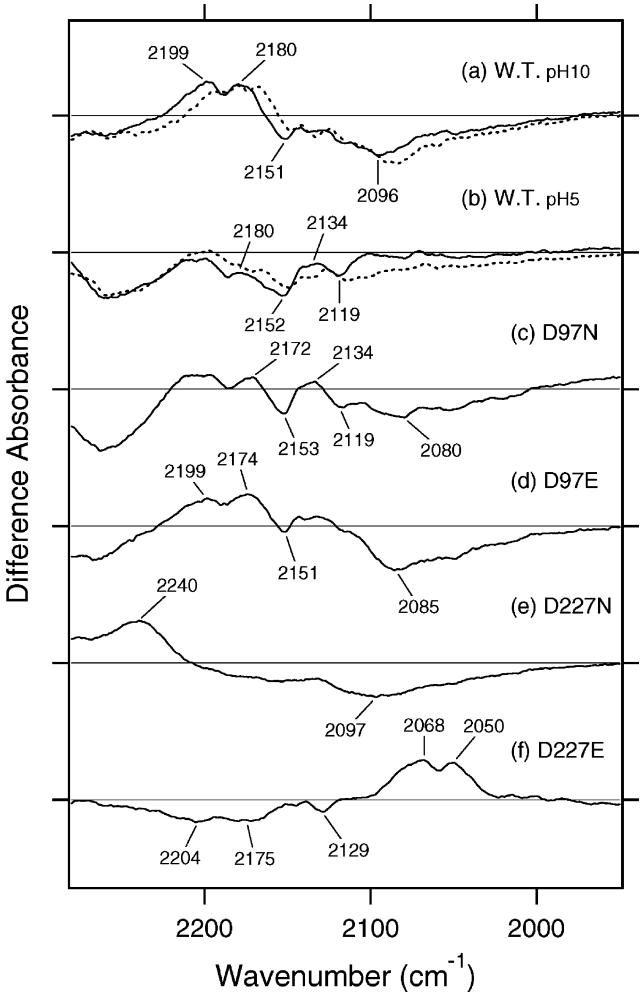

FIGURE 5: PR_K minus PR difference infrared spectra of the wild-type (pH 10; a, and pH 5; b), D97N (c), D97E (d), D227N (e), and D227E (f) PR in the 2280−1950 cm^{-1} region. The samples were hydrated with D_2O, and spectra were measured at 77 K. The solid lines (—) represent the measurements for the unlabeled samples, whereas the dotted lines (····) in a and b represent the measurements for the [ζ-^{15}N]Lys-labeled samples. One division of the *y*-axis corresponds to 0.0004 units.

after photoisomerization. The corresponding frequency differences in the wild type at pH 5 were 28 and 20 cm^{-1} for PR_K and PR, respectively (Figure 4b). The values were 28 (PR_K) and 31 (PR) cm^{-1} for D97N (Figure 4c), 28 (PR_K) and 30 (PR) cm^{-1} for D97E (Figure 4d), 9 (PR_K) and 23 (PR) cm^{-1} in D227N (Figure 4e), and 24 (PR_K) and 30 (PR) cm^{-1} in D227E (Figure 4f). According to the results, the frequency differences in the unphotolyzed PR state range between 20 and 31 cm^{-1}, providing similar hydrogen-bonding strengths. In contrast, the value in PR_K of D227N (9 cm^{-1}) is remarkably smaller than that for the others (24−29 cm^{-1}). It suggests that PR_K of D227N lacks a hydrogen bond of the Schiff base. Interaction of the Schiff base with Asp227 in PR_K is consistent with the results for the COO^- stretching (Figure 2) and HOOP (Figure 3) vibrations. It should, however, be noted that the C═N stretch is not the direct measure of the hydrogen-bonding strength of the Schiff base, and other signals such as amide-I vibrations may hamper accurate interpretation. A more direct probe of the hydrogen-bonding strength of the protonated Schiff base is the N−H stretch. Therefore, we examined the hydrogen-bonding strength of the Schiff base again by an analysis of the N−D stretch vibrations in D_2O.

N−D Stretching Vibrations of the Protonated Schiff Base. Figure 5 shows the PR_K minus PR difference infrared spectra of the wild-type (pH 10; a, and pH 5; b), D97N (c), D97E (d), D227N (e), and D227E (f) PR in D_2O at 2280−1950 cm^{-1}. The bands at 2199(+), 2180(+), 2151(−), and 2096(−) cm^{-1} in the wild type at pH 10 exhibit downshift for the [ζ-^{15}N]Lys-labeled sample (Figure 5a), indicating that the bands originate from the N−D stretch of the Schiff base. The N−D stretches in PR at 2151 and 2096 cm^{-1} are comparable to those in BR (2173 and 2123 cm^{-1}) (*38*), and the upshift of the N−D stretch upon PR_K formation indicates a weakened hydrogen bond of the Schiff base after retinal isomerization, as is the case in BR. However, it should be noted that the frequency changes are much smaller in PR_K (2199 and 2180 cm^{-1}) than in BR_K (2495 and 2468 cm^{-1}) (*24*). This indicates that the Schiff base still forms a hydrogen bond in PR_K. The spectral upshift of the N−D stretch is further reduced at acidic pH in the wild type. Figure 5b identifies the N−D stretching vibrations at 2180 and 2129 cm^{-1} for PR_K, and at 2152 and 2119 cm^{-1} for PR in its acidic form.

Spectral features in D97N are similar to those of the wild type at pH 5. D97N possesses bands at 2172(+), 2153(−), 2134(+), and 2119(−) cm^{-1} (Figure 5c), which presumably correspond to those at 2180(+), 2152(−), 2134(+), and 2119(−) cm^{-1} in the wild type at pH 5 (Figure 5b). Spectral features in D97E are also similar to those of the wild type at pH 10. D97E possesses bands at 2199(+), 2174(+), 2151(−), and 2085(−) cm^{-1} (Figure 5d), which presumably correspond to those at 2199(+), 2180(+), 2151(−), and 2096(−) cm^{-1} in the wild type at pH 10 (Figure 5a). Therefore, protonation of Asp97 affects the hydrogen-bonding alteration of the Schiff base as is obvious from a comparison of Figure 5a and b. Nevertheless, the similar spectra of D97E and the wild type (pH 10) suggest that Asp97 plays a minor role in the changes of the hydrogen-bonding network before and after retinal isomerization.

However, entirely different spectra were obtained for the mutants of Asp227. In the case of D227N, there is only a positive peak at 2240 cm^{-1}, and a broad negative band was observed at 2200−2000 cm^{-1} (Figure 5e). The positive and negative bands in Figure 5e seem to be widely separated, and the N−D stretch of the Schiff base is probably at 2240 and 2097 cm^{-1} for PR_K and PR, respectively, in D227N. This observation indicates that the hydrogen bond of the Schiff base is considerably weakened upon PR_K formation, which is consistent with the interpretation from the C=N stretch (Figure 4e). The weakened hydrogen bond of the Schiff base in D227N suggests that the Schiff base somehow interacts with Asp227 in PR_K. Interestingly, the spectral features in Figure 5f look opposite to those in Figure 5a, exhibiting spectral downshift, not upshift, upon PR_K formation in D227E. The N−D stretches of the Schiff base in D227E are presumably located at 2204, 2175, and 2129 cm^{-1} for PR, and at 2068 and 2050 cm^{-1} for PR_K. The results on the mutants of Asp97 and Asp227 strongly suggest that the Schiff base interacts with Asp227 in the K intermediate.

O−D Stretching Vibrations of Internal Water Molecules. Figure 6 shows the PR_K minus PR difference infrared spectra of the wild-type (pH 10; a, and pH 5; b), D97N (c), D97E (d), D227N (e), and D227E (f) PR in D_2O at 2740−2200 cm^{-1}. This frequency region includes the X−D stretching vibrations of protein and water molecules, the latter of which can be assigned by using $D_2{}^{18}O$. The green-labeled frequencies correspond to those identified as water stretching vibrations. In the wild type at pH10, four negative peaks at 2683, 2667, 2463, and 2315 cm^{-1} were assigned earlier to the vibrations of water molecules (Figure 6a) (*25*), among which the frequency of the band at 2315 cm^{-1} is much lower than those of fully hydrated tetrahedral water molecules (*18*). Such a strongly hydrogen-bonded water molecule was not observed for the wild type at pH 5 (Figure 6b). Instead, a new negative band appears at 2582 cm^{-1}, suggesting that the water near Asp97 possesses an O−D stretch at 2315 or 2582 cm^{-1} depending on pH.

Among the mutant proteins, D97N and D227N do not possess water O−D stretches at <2400 cm^{-1} (Figure 6c and e), indicating that they lack strongly hydrogen-bonded water molecules. Similar observations were made for the D85N and D212N mutant BR (*20*, *21*). However, D97E possess a negative water band at 2300 cm^{-1} (Figure 6d). The similar but a slightly lower frequency than that in the wild type (2315 cm^{-1}) implies that the water molecule is located near Asp97, and the stronger hydrogen bond of the water molecule may originate from the shortened distance from the carboxylic oxygen of Glu97.

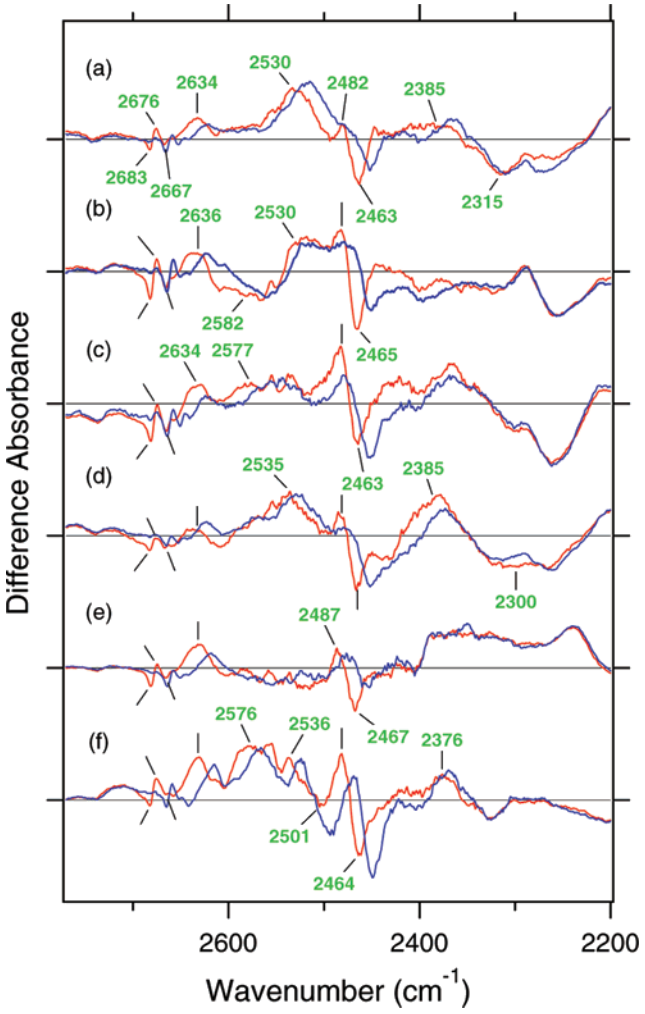

FIGURE 6: PR_K minus PR difference infrared spectra of the wild-type (pH 10; a, and pH 5; b), D97N (c), D97E (d), D227N (e), and D227E (f) PR in the 2740−2200 cm^{-1} region. The samples were hydrated with D_2O (red lines) or $D_2{}^{18}O$ (blue lines), and spectra were measured at 77 K. The green-labeled frequencies correspond to those identified as water stretching vibrations. One division of the *y*-axis corresponds to 0.00055 absorbance units.

Four positive peaks at 2676, 2634, 2530, and 2385 cm^{-1} in Figure 6a were assigned earlier to the vibrations of water molecules in PR_K of the alkaline form (*25*). In addition, here we identified the band at 2482 cm^{-1} (Figure 6a) as an O−D stretch of water by analyzing the results from the mutants (Figure 6c−f). Considering strongly hydrogen-bonded water molecules, a positive band at 2385 cm^{-1} in the alkaline PR (Figure 6a) disappears upon the neutralization of Asp97 (Figure 6c) or Asp227 (Figure 6e), whereas it appears at the same frequency in D97E (Figure 6d) or at a slightly lower frequency in D227E (2376 cm^{-1}; Figure 6f). This observation may indicate that such a strongly hydrogen-bonded water molecule interacts with Asp227, not Asp97, in the K state of PR. The water bands at 2683(−), 2676(+), 2667(−), 2634(+), 2482(+), and 2463(−) cm^{-1} in Figure 6a were observed in all mutants. Therefore, such water molecules are not located in the vicinity of Asp97 and Asp227. PR may have water molecules in the cytoplasmic region, though

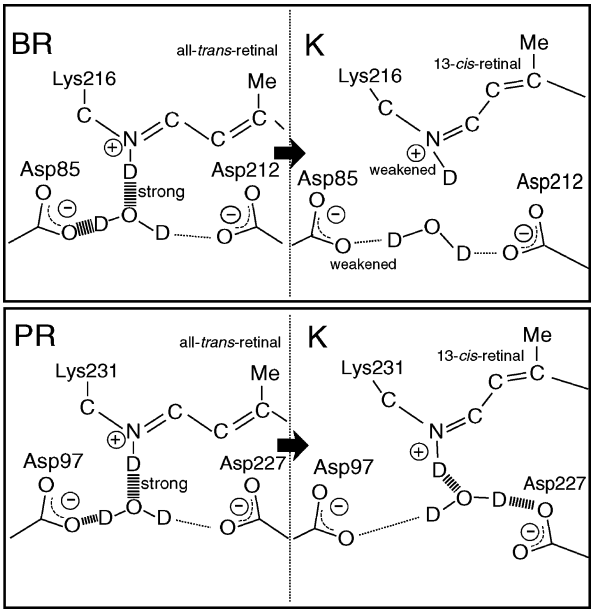

FIGURE 7: Schematic drawing of the hydrogen-bonding interactions of the Schiff base and water molecule with the counterion on the basis of the present FTIR results. The stacked bars indicate strong hydrogen bonds. The bridged water molecule interacts with D227 in the K intermediate of PR.

BR has only two water molecules (*22*), and they do not change in the BR-to-K transition (*21*).

Another noteworthy observation is the absence of the band due to Thr101. In the BR_K minus BR difference infrared spectra, there are sharp peaks at 2506(−)/2466(+) cm^{-1}, which were identified as the O−D stretches of Thr89 (*39*, *40*). From the frequency and dichroic properties of the O−D stretch, we revealed a strong interaction of the O−D group of Thr89 with Asp85, and such strong interactions between Thr89 and Asp85 must contribute to the lowering of the pK_a of Asp85 in BR. In fact, the pK_a of Asp85 in T89A mutant BR was reported to be 4.4 in DMPC/CHAPS micelles, being about 1 unit higher than that of the wild-type BR in the micelles (3.5) (*41*). Figure 6a shows the lack of such bands for PR in the 2700−2400 cm^{-1} region, where most bands can be assigned as water O−D stretches. Because threonine is conserved in PR (Thr101), this fact suggests the absence of strong interaction between Thr101 and Asp97 in PR. This is probably one of the structural reasons for the higher pK_a value of Asp97.

DISCUSSION

In this work, we studied the structural changes of PR following retinal photoisomerization by means of low-temperature Fourier-transform infrared (FTIR) spectroscopy at 77 K. We assigned the Schiff base N−D stretches and water O−D stretches in the PR_K minus PR difference spectra by using [ζ-^{15}N]Lys-labeling and ^{18}O water, respectively. We also measured FTIR spectra of the mutants of Asp97 (D97N and D97E) and Asp227 (D227N and D227E) for a detailed structural analysis. Interestingly, the PR_K minus PR spectra of the wild type were similar to those of D97N and D97E but different from those of D227N and D227E. On the basis of the present FTIR observations, we discuss the structure and structural changes in the Schiff base region by comparing those of BR (Figure 7).

Unphotolyzed States of PR and BR. The λ_{max} of the wild-type, D97N, and D227N mutant PR were located at 523, 548, and 523 nm in DM solution (pH 9), clearly indicating that Asp97 is the principal counterion of the protonated Schiff base, as is the case in BR. The spectral blue shift in D227E by 15 nm suggests that Asp227 is also involved in the counterion complex. Therefore, the structure in the Schiff base region is likely to be similar for PR and BR. In the case of BR, a water molecule is located among the Schiff base, Asp85, and Asp212 (*22*), but our FTIR study revealed that the water bridges the Schiff base and Asp85 through a strong hydrogen-bonding interaction (Figure 7) (*20*, *21*). The similarity of the N−D stretches of the Schiff base in PR to those in BR strongly suggests that the protonated Schiff base in PR forms a strong hydrogen bond, presumably with a water molecule. The strongly hydrogen-bonded water molecule, whose O−D stretch is located at 2315 cm^{-1}, disappears upon the protonation of Asp97 (pH 5) and upon the mutation of Asp97 into asparagine (Figure 6). The O−D stretch at 2171 cm^{-1} in BR also disappears in the D85N mutant (*20*, *21*). From these facts, we propose that PR possesses a bridged water molecule between the Schiff base and Asp97 similar to BR (Figure 7). Although the hydrogen-bonding strength of the Schiff base with water is similar for BR and PR, that of water with Asp97 and Asp85 is weaker in PR than in BR as seen from the frequency of water O−D stretches (2315 vs 2171 cm^{-1}). The weaker association of the water with Asp97 probably contributes to its higher pK_a (∼7), along with the weaker association of Thr101 to Asp97 compared to that of Thr89 in BR (*39*, *41*).

In addition to the bridged water, two more water molecules constitute the hydrogen-bonding network in the Schiff base region of BR (*22*). Each water molecule possesses a strong hydrogen bond as shown by the O−D stretch at 2292 and 2323 cm^{-1} (*21*), and such a water-containing hydrogen-bonding network must play crucial role in BR. In fact, these water bands are highly influenced by mutations at the extracellular domain of BR (*21*). In contrast, several water bands were insensitive to the mutations of Asp97 and Asp227 in PR. This may suggest that the water molecules with O−D stretches at 2683(−), 2676(+), 2667(−), 2634(+), 2482(+), and 2463(−) cm^{-1} (Figure 6a) originate from the cytoplasmic region.

K Intermediate of PR and BR after Retinal Photoisomerization. The N−D stretch of the Schiff base is upshifted by ∼350 cm^{-1} in BR_K (∼550 cm^{-1} as the N−H stretch), indicating that the hydrogen bond is lost after retinal photoisomerization in BR (*38*). A considerably different picture was obtained for PR in the present study. PR (at pH 10) also exhibits the upshift of the N−D stretch, but the value is <100 cm^{-1} (Figure 5a), indicating that the Schiff base keeps a hydrogen bond after retinal photoisomerization. What is the hydrogen-bonding acceptor of the Schiff base in PR_K? The present mutation study provided information on the interaction partner of the Schiff base in PR_K. The D227 mutations (D227N and D227E) remarkably affect the Schiff base, whereas negligible effects were observed for the D97 mutants (D97N and D97E). These results strongly suggest that the Schiff base interacts with Asp227 in PR_K. Although it is possible that the protonated Schiff base directly interacts with Asp227, we propose that the Schiff base forms a

hydrogen bond with a water, which further forms a hydrogen bond with Asp227, as follows from the analysis of water O−D stretches in Figure 6. According to the scheme in Figure 7, photoisomerization should move the Schiff base toward Asp227 in PR. Such retinal motion has been reported for the MD simulation of the primary photoreaction in BR (*42*). Therefore, a similar motion of the Schiff base probably takes place in PR, although the Schiff base still forms a hydrogen bond after such motion. An important role for Asp227 was also reported by the observation of the increased concentration of the 9-cis form in D227N (*43*).

REFERENCES

1. Haupts, U., Tittor, J., and Oesterhelt, D. (1999) Closing in on bacteriorhodopsin: progress in understanding the molecules, *Annu. Rev. Biophys. Biomol. Struct. 28*, 367−399.
2. Lanyi, J. K. (2000) Molecular mechanism of ion transport in bacteriorhodopsin: insights from crystallographic, spectroscopic, kinetic, and mutational studies, *J. Phys. Chem. B 104*, 11441−11448.
3. Kandori, H. (2000) Role of internal water molecules in bacteriorhodopsin, *Biochim. Biophys. Acta 1460*, 177−191.
4. Bieszke, J. A., Braun, E. L., Bean, L. E., Kang, S., Natvig, D. O., and Borkovich, K. A. (1999) The nop-1 gene of neurospora crassa encodes a seven transmembrane helix retinal-binding protein homologous to archaeal rhodopsins, *Proc. Natl. Acad. Sci. U.S.A. 96*, 8034−8039.
5. Sineshchekov, O. A., Jung, K. H., and Spudich, J. L. (2002) Two rhodopsins mediate phototaxis to low- and high-intensity light in *Chlamydomonas reinhardtii*, *Proc. Natl. Acad. Sci. U.S.A. 99*, 8689−8694.
6. de la Torre, J. R., Christianson, L. M., Beja, O., Suzuki, M. T., Karl, D. M., Heidelberg, J., and DeLong, E. F. (2003) Proteorhodopsin genes are distributed among divergent marine bacterial taxa, *Proc. Natl. Acad. Sci. U.S.A. 100*, 12830−12835.
7. Jung, K. H., Trivedi, V. D., and Spudich, J. L. (2003) Demonstration of a sensory rhodopsin in eubacteria, *Mol. Microbiol. 47*, 1513−1522.
8. Brown, L. S., and Jung, K. H. (2006) Bacteriorhodopsin-like proteins of eubacteria and fungi: the extent of conservation of the haloarchaeal proton-pumping mechanism, *Photochem. Photobiol. Sci. 5*, 538−546.
9. Beja, O., Aravind, L., Koonin, E. V., Suzuki, M. T., Hadd, A., Nguyen, L. P., Jovanovich, S. B., Gates, C. M., Feldman, R. A., Spudich, J. L., Spudich, E. N., and DeLong, E. F. (2000) Bacterial rhodopsin: evidence for a new type of phototrophy in the sea, *Science 289*, 1902−1906.
10. Beja, O., Spudich, E. N., Spudich, J. L., Leclerc, M., and DeLong, E. F. (2001) Proteorhodopsin phototrophy in the ocean, *Nature 411*, 786−789.
11. Sabehi, G., Loy, A., Jung, K. H., Partha, R., Spudich, J. L., Isaacson, T., Hirschberg, J., Wagner, M., and Beja, O. (2005) New insights into metabolic properties of marine bacteria encoding proteorhodopsins, *PLoS Biol. 3*, e273.
12. Dioumaev, A. K., Brown, L. S., Shih, J., Spudich, E. N., Spudich, J. L., and Lanyi, J. K. (2002) Proton transfers in the photochemical reaction cycle of proteorhodopsin, *Biochemistry 41*, 5348−5358.
13. Friedrich, T., Geibel, S., Kalmbach, R., Chizhov, I., Ataka, K., Heberle, J., Engelhard, M., and Bamberg, E. (2002) Proteorhodopsin is a light-driven proton pump with variable vectoriality, *J. Mol. Biol. 321*, 821−838.
14. Dioumaev, A. K., Wang, J. M., Balint, Z., Varo, G., and Lanyi, J. K. (2003) Proton transport by proteorhodopsin requires that the retinal schiff base counterion Asp-97 be anionic, *Biochemistry 42*, 6582−6587.
15. Sineshchekov, O. A., and Spudich, J. L. (2004) Light-induced intramolecular charge movement in microbial rhodopsins in intact E. coli cells, *Biophys. J. 3*, 548−554.
16. Lakatos, M., Lanyi, J. K., Szakacs, J., and Varo, G. (2003) The photochemical reaction cycle of proteorhodopsin at low pH, *Biophys. J. 84*, 3252−3256.
17. Varo, G., Brown, L. S., Lakatos, M., and Lanyi, J. K. (2003) Characterization of the photochemical reaction cycle of proteorhodopsin, *Biophys. J. 84*, 1202−1207.
18. Furutani, Y., and Kandori, H. (2002) Internal water molecules of archaeal rhodopsins, *Mol. Membr. Biol. 19*, 257−265.
19. Kandori, H., and Shichida, Y. (2000) Direct observation of the bridged water stretching vibrations inside a protein, *J. Am. Chem. Soc. 122*, 11745−11746.
20. Shibata, M., Tanimoto, T., and Kandori, H. (2003) Water molecules in the schiff base region of bacteriorhodopsin, *J. Am. Chem. Soc. 125*, 13312−13313.
21. Shibata, M., and Kandori, H. (2005) FTIR studies of internal water molecules in the Schiff base region of bacteriorhodopsin, *Biochemistry 44*, 7406−7413.
22. Luecke, H., Schobert, B., Richter, H.-T., Cartailler, J.-P., and Lanyi, J. K. (1999) Structure of bacteriorhodopsin at 1.55 Å resolution, *J. Mol. Biol. 291*, 899−911.
23. Hayashi, S., and Ohmine, I. (2000) Proton transfer in bacteriorhodopsin: structure, excitation, IR spectra, and potential energy surface analyses by an ab initio QM/MM method, *J. Phys. Chem. B 104*, 10678−10691.
24. Furutani, Y., Shibata, M., and Kandori, H. (2005) Strongly hydrogen-bonded water molecules in the Schiff base region of rhodopsins, *Photochem. Photobiol. Sci. 4*, 661−666.
25. Furutani, Y., Ikeda, D., Shibata, M., and Kandori, H. (2006) Strongly hydrogen-bonded water molecule is observed only in the alkaline form of proteorhodopsin, *Chem. Phys. 324*, 705−708.
26. Bergo, V., Amsden, J. J., Spudich, E. N., Spudich, J. L., and Rothschild, K. J. (2004) Structural changes in the photoactive site of proteorhodopsin during the primary photoreaction, *Biochemistry 43*, 9075−9083.
27. Krebs, R. A., Alexiev, U., Partha, R., DeVita, A. M., and Braiman, M. S. (2002) Detection of fast light-activated H^+ release and M intermediate formation from proteorhodopsin, *BMC Physiol. 2*, 5.
28. Furutani, Y., Kamada, K., Sudo, Y., Shimono, K., Kamo, N., and Kandori, H. (2005) Structural changes of the complex between pharaonis phoborhodopsin and its cognate transducer upon formation of the M photointermediate, *Biochemistry 44*, 2909−2915.
29. Sudo, Y., Furutani, Y., Shimono, K., Kamo, N., and Kandori, H. (2003) Hydrogen bonding alteration of Thr-204 in the complex between pharaonis phoborhodopsin and its transducer protein, *Biochemistry 42*, 14166−14172.
30. Imasheva, E. S., Shimono, K., Balashov, S. P., Wang, J. M., Zadok, U., Sheves, M., Kamo, N., and Lanyi, J. K. (2005) Formation of a long-lived photoproduct with a deprotonated Schiff base in proteorhodopsin, and its enhancement by mutation of Asp227, *Biochemistry 44*, 10828−10838.
31. Furutani, Y., Bezerra, A. G., Jr., Waschuk, S., Sumii, M., Brown, L. S., and Kandori, H. (2004) FTIR spectroscopy of the K photointermediate of neurospora rhodopsin: structural changes of the retinal, protein, and water molecules after photoisomerization, *Biochemistry 43*, 9636−9646.
32. Mogi, T., Stern, L. J., Marti, T., Chao, B. H., and Khorana, H. G. (1988) Aspartic acid substitutions affect proton translocation by bacteriorhodopsin, *Proc. Natl. Acad. Sci. U.S.A. 85*, 4148−4152.
33. Xiao, Y., Partha, R., Krebs, R., and Braiman, M. (2005) Time-resolved FTIR spectroscopy of the photointermediates involved in fast transient H^+ release by proteorhodopsin, *J. Phys. Chem. B 109*, 634−641.
34. Krebs, R. A., Dunmire, D., Partha, R., and Braiman, M. S. (2003) Resonance Raman characterization of proteorhodopsin's chromophore environment, *J. Phys. Chem. B 107*, 7877−7883.
35. Mathies, R. A., Smith, S. O., and Palings, I. (1987) In *Biological Applications of Raman Spectroscopy: Resonance Raman Spectra of Polyenes and Aromatics* (Spiro, T. G., Ed.) pp 59−108, John Wiley and Sons, New York.
36. Furutani, Y., Sudo, Y., Wada, A., Ito, M., Shimono, K., and Kandori, H. (2006) Assignment of the hydrogen-out-of-plane vibrations of the retinal chromophore in the K intermediate of *Pharaonis* phoborhodopsin, *Biochemistry 45*, 11836−11843.
37. Baasov, T., Friedman, N., and Sheves, M. (1987) Factors affecting the C═N stretching in protonated retinal schiff base: a model study for bacteriorhodopsin and visual pigments, *Biochemistry 26*, 3210−3217.
38. Kandori, H., Belenly, M., and Herzfeld, J. (2002) Vibrational frequency and dipolar orientation of the protonated Schiff base in bacteriorhodopsin before and after photoisomerization, *Biochemistry 41*, 6026−6031.

39. Kandori, H., Kinoshita, N., Yamazaki, Y., Maeda, A., Shichida, Y., Needleman, R., Lanyi, J. K., Bizounok, M., Herzfeld, J., Raap, J., and Lugtenburg, J. (1999) Structural change of threonine 89 upon photoisomerization in bacteriorhodopsin as revealed by polarized FTIR spectroscopy, *Biochemistry 38*, 9676−9683.
40. Kandori, H., Yamazaki, Y., Shichida, Y., Raap, J., Lugtenburg, J., Belenky, M., and Herzfeld, J. (2001) Tight Asp-85−Thr-89 association during the pump switch of bacteriorhodopsin, *Proc. Natl. Acad. Sci. U.S.A. 98*, 1571−1576.
41. Marti, T., Otto, H., Mogi, T., Rosselet, S. J., Heyn, M. P., and Khorana, H. G. (1990) Bacteriorhodopsin mutants containing single substitutions of serine or threonine residues are all active in proton translocation, *J. Biol. Chem. 266*, 6919−6927.
42. Hayashi, S., Tajkhorshid, E., and Schulten, K. (2003) Molecular dynamics simulation of bacteriorhodospin's photoisomerization using ab initio forces for the excited chromophore, *Biophys. J. 85*, 1440−1449.
43. Imasheva, E. S., Balashov, S. P., Wang, J. M., Dioumaev, A. K., and Lanyi, J. K. (2004) Selectivity of retinal photoisomerization in proteorhodopsin is controlled by aspartic acid 227, *Biochemistry 43*, 1648−1655.
44. Needleman, R., Chang, M., Ni, B., Varo, G., Fornes, J., White, S. H., and Lanyi, J. K. (1991) Properties of $Asp^{212} \rightarrow Asn$ bacteriorhodopsin suggest that Asp^{212} and Asp^{85} both participate in a counterion and proton acceptor complex near the schiff base, *J. Biol. Chem. 266*. 11478−11484.

BI700143G